Experimental Warming Leads to Convergent Succession of Grassland Archaeal

2 Community

3 4

1

- 5 Ya Zhang¹, Daliang Ning¹, Linwei Wu^{1,2}, Mengting Maggie Yuan^{1,3}, Xishu Zhou^{1,4}, Xue Guo⁵,
- 6 Yuanliang Hu^{1,6}, Siyang Jian¹, Zhifeng Yang¹, Shun Han¹, Jiajie Feng¹, Jialiang Kuang¹, Carolyn
- 7 R. Cornell¹, Colin T. Bates¹, Yupeng Fan¹, Jonathan P. Michael¹, Yang Ouyang¹, Jiajing Guo^{1,7},
- 8 Zhipeng Gao^{1,8}, Zheng Shi¹, Naijia Xiao¹, Ying Fu¹, Aifen Zhou¹, Liyou Wu¹, Xueduan Liu⁴,
- 9 Yunfeng Yang⁵, James M. Tiedje⁹, and Jizhong Zhou^{1,10,11,12,§}

- 11 ¹Institute for Environmental Genomics and Department of Microbiology and Plant Biology,
- 12 University of Oklahoma, Norman, OK, USA;
- ²Institute of Ecology, Key Laboratory for Earth Surface Processes of the Ministry of Education,
- 14 College of Urban and Environmental Sciences, Peking University, Beijing, China;
- 15 ³Department of Environmental Science, Policy, and Management, University of California,
- 16 Berkeley, CA, USA;
- ⁴School of Minerals Processing and Bioengineering, Central South University, Changsha, Hunan,
- 18 China;
- 19 ⁵State Key Joint Laboratory of Environment Simulation and Pollution Control, School of
- 20 Environment, Tsinghua University, Beijing, China;
- ⁶Hubei Key Laboratory of Edible Wild Plants Conservation & Utilization, College of Life Sciences,
- 22 Hubei Normal University, Huangshi, China
- ⁷Hunan Agriculture Product Processing Institute, Hunan Academy of Agricultural Sciences,
- 24 Changsha, Hunan, China;
- ⁸College of Animal Science and Technology, Hunan Agricultural University, Changsha, Hunan,
- 26 China;
- ⁹Center for Microbial Ecology, Michigan State University, East Lansing, MI, USA;
- 28 ¹⁰School of Civil Engineering and Environmental Sciences, University of Oklahoma, Norman, OK,
- 29 USA;
- 30 ¹¹School of Computer Science, University of Oklahoma, Norman, OK, USA

31	¹² Earth and Environmental Sciences, Lawrence Berkeley National Laboratory, Berkeley, CA								
32	USA.								
33									
34	§Corresponding author: Dr. Jizhong Zhou								
35	Institute for Environmental Genomics (IEG)								
36	Department of Microbiology and Plant Biology								
37	University of Oklahoma								
38	Norman, OK 73019								
39	Phone: 405.325.6073								
40	Fax: 405-325-7552								
41	E-mail: jzhou@ou.edu								

43 Abstract

Understanding the temporal succession of ecological communities and the underlying mechanisms in response to climate warming is critical for future climate projections. However, despite its fundamental importance in ecology and evolution, little is known about how the Archaea domain responds to warming. Here, we showed that experimental warming of a tallgrass prairie ecosystem significantly altered the community structure of soil archaea and reduced their taxonomic and phylogenetic diversity. In contrast to previous observations in bacteria and fungi, we showed convergent succession of the soil archaeal community between warming and control. Although stochastic processes dominated the archaeal community, their relative importance decreased over time. Furthermore, the warming-induced changes in the archaeal community and soil chemistry had significant impacts on ecosystem functioning. Our results imply that, although the detrimental effects of biodiversity loss on ecosystems could be much severer, the soil archaeal community structure would be more predictable in a warmer world.

Since its formal recognition in 1990¹, the archaea domain has challenged our views on the diversity, ecology, and evolution of life, yet remains the least understood². In contrast to the traditional wisdom that archaea prefer extreme environments³⁻⁵, archaea are prominent members of all terrestrial and marine communities² and are abundant in water columns, ocean sediments, and soils^{5, 6}. Possessing unusual physiologies^{2, 7}, they play central roles in mediating global carbon (C), nitrogen (N), and sulfur (S) cycles⁸⁻¹⁰. They are also an important component of the human microbiome, though their role in health and disease remains undetermined¹¹.

Furthermore, the recent discovery of the Asgard archaeal superphylum leads to a possibility of archaea as ancestors of eukaryotic life¹²⁻¹⁴. Thus, understanding the physiology, ecology and evolution of archaea represents one of the most exciting frontiers in biology².

Despite such recent exciting discoveries, we have a limited understanding of archaea in terrestrial environments, particularly in soils^{6, 15-18}. Archaea are ubiquitously present in soil, represent a mass of 0.5 Gt C (a comparable amount with 7 Gt C for soil bacteria)¹⁸, and are vital to soil nitrification and methanogenesis due to the high numbers of ammonia-oxidizing archaea (AOA) and methanogenic archaea^{19, 20}. It was reported that their spatial distribution patterns in soils are distinct from those of soil bacteria^{6, 15}, including biodiversity distribution and ecological drivers^{6, 15-17}. However, our understanding of the responses of soil archaea to climate change remains rudimentary²¹⁻²⁴.

Climate warming represents one of the biggest disturbance factors imposed on human society and global ecosystems. As temperature is a major driver of biological processes, climate warming will impact various ecological communities. Based on long-term time-series data, our

previous studies revealed that experimental warming leads to the divergent succession of soil bacterial and fungal communities²⁵, accelerates microbial temporal scaling²⁶, reduces the biodiversity of soil bacteria, fungi, and protists²⁷, but increases bacterial network complexity and stability²⁸. However, how climate warming affects the temporal succession of the archaeal community remains elusive. On the one hand, since archaea and bacteria are both prokaryotic and share greater structural similarity²⁹, it is expected that climate warming could lead to the divergent succession of soil archaeal communities similarly as it does for bacteria and fungi. On the other hand, soil archaeal communities could exhibit distinct temporal responses to climate warming as convergent or idiosyncratic³⁰ since archaea have unique physiology⁷.

Here, we conducted a long-term *in situ* warming experiment in a native, tallgrass prairie ecosystem at the Kessler Atmospheric and Ecological Field Station (KAEFS) in the US Great Plains in Central Oklahoma (34° 59′ N, 97° 31′ W)^{25, 31}. This long-term multifactor climate change experiment was established in 2009 with a split-block design, in which the warming treatment plots have been subjected to continuous + 3 °C warming by infrared radiators and the control plots by "dummy" infrared radiators to account for the shading effect³¹. In this study, we focus on the warming effects on soil archaeal community diversity and succession by determining: (i) whether and how warming affects the diversity and succession of soil archaeal community; (ii) what the relative roles of deterministic and stochastic processes are in controlling the temporal dynamics of soil archaeal community in response to climate warming; and (iii) whether and how warming-induced changes of soil archaeal community mediate ecosystem functioning. We hypothesize that soil archaeal community would undergo divergent succession under warming due to increased deterministic filtering effects over time, similar to

what was observed for bacteria and fungi, and that decreases in the taxonomical and functional diversity of soil archaeal community under warming would negatively impact linked ecosystem functions.

Impacts of warming on archaeal diversity. At the higher taxonomical levels, such as phylum and order, the soil archaeal community was primarily composed of Thaumarchaeota (Nitrososphaerales; $\geq 96.5\%$ in abundance, $\geq 41.3\%$ in incidence) and Euryarchaeota (Methanomassiliicoccales; $\sim 0.35\%$ in abundance, $\sim 2.1\%$ in incidence), and to a lesser extent of Pacearchaeota (unclassified), Woesearchaeota (unclassified), and Crenarchaeota (unclassified) (Fig. 1a, Extended Data Fig. 1). The major Nitrososphaerales clade identified was potentially responsible for ammonia oxidation process³², and the Methanomassiliicoccales clade was potential methanogens³³.

To examine the warming effects on soil archaeal community diversity, linear mixed-effects models (LMM) were used, in which the regression coefficients represent the directions and magnitudes of the warming effect, namely effect sizes (β). Warming had strong negative effects (β = -0.64 \sim - 0.60, p < 0.008) on archaeal richness and Faith's phylogenetic diversity (PD) (Fig. 1b), as richness decreased by 1.4% (β = -0.64, p = 0.008) and PD by 7.3% (β = -0.60, p = 0.006). Similarly, warming also decreased the functional richness of the archaeal community measured by a probebased microarray GeoChip (β = -0.17, p = 0.070). However, such decreases in functional richness were not detected by metagenome EcoFUN-MAP (β = 0.14, p = 0.533; Fig. 1b), which was most likely due to the inherent problems of lower reproducibility, quantitative capability and sensitivity associated with shotgun sequencing approaches³⁴⁻³⁶. These results indicate that experimental

warming significantly reduced soil archaeal biodiversity, consistent with the observations for bacteria, fungi, and protists^{27, 37-39}.

The warming effects on soil archaea varied considerably for individual operational taxonomic units (OTUs). Warming significantly decreased the relative abundance of Nitrososphaerales-affiliated OTU2 (response ratios (RR) = -0.45 \pm 0.32; 9.1% under warming vs 14.3% under control; Supplementary Table S1), but increased the relative abundance of other Nitrososphaerales-affiliated taxa, including OTU4 (RR = 0.40 \pm 0.27; 10.9% vs 7.4%) and OTU11 (RR = 0.75 \pm 0.60; 1.3% vs 0.6%). Two rare Methanobacteriales-affiliated taxa (OTU1057 and OTU535) were significantly negatively impacted by warming (RR < -2.30; <0.001% under warming vs. 0.01% under control). These results suggest high variability even within the same taxonomical clade in responses to warming, consistent with our previous observations on the differential effects of warming on various microbial groups of bacteria and fungi²⁵.

Effects of warming on community structure and succession. As revealed by three complementary non-parametric multivariate statistical tests (Adonis, ANOSIM, and MRPP), the overall archaeal community structure was significantly different (p < 0.05) between the warmed and control plots (Table 1, Supplementary Table S2). Time also had significant (p < 0.03) effects on the soil archaeal community (Table 1). The detrended correspondence analysis (DCA) showed that the soil archaeal community structure was shifted over time by warming (Extended Data Fig. 2). Before starting warming treatment in 2009, the soil samples from both warmed and control plots were closely clustered. In the subsequent years, the warmed samples were generally

separated from the control samples on a yearly basis (Extended Data Fig. 2). Together, these results suggest that experimental warming significantly altered soil archaeal community structure and succession, which agrees with the results for bacteria and fungi observed in this site²⁵. Studies with plants have shown similar results with climate warming impacting phylogenetic diversity of grassland plant communities³⁹, abundance within species ranges of trees⁴⁰, and local species extinctions of plants⁴¹.

The community differences between the paired warmed and control plots decreased significantly with time based on both the Sorensen metric (Fig. 1c; slope = -0.009, p = 0.043) and phylogenetic distance metric (Fig. 1c; slope = -0.013, p = 0.020). In contrast, the corresponding community differences between warming and control increased with time for bacteria (Fig. 1c; slope = 0.011, p = 0.004 for Sorensen metrics and slope = 0.009, p = 0.001 for unweighted Unifrac metrics), and fungi (Extended Data Fig. 3; slope = 0.020, p = 0.007 for Sorensen metrics and slope = 0.014, p = 0.003 for unweighted Unifrac metrics). Also, both potential ammonia oxidizer (Nitrososphaerales) and the dominant methanogen (Methanomassiliicoccales) showed similar trends as the domain Archaea (Extended Data Fig. 4). In addition, the archaeal functional gene-based (amoA gene) community distances between warming and control decreased significantly (p < 0.05) over time (Fig. 1d). All these results suggest the convergent succession of the soil archaeal community between warming and control, which is opposite to those observed in bacteria.

The contrasting directions of succession between the domains of Archaea and Bacteria in response to experimental warming invalidated our hypothesis of similar succession patterns

between the two domains. The opposite directions in succession between soil archaea and bacteria could be due to distinctions in biochemistry, genetics, physiology, ecology, and evolution 42, 43. For instance, the soil archaeal community has relatively low taxonomic and phylogenetic diversity (primarily Nitrososphaerales). These detected archaeal species are also functionally similar with narrow ecological niches (i.e., nitrification) and are replacing each other over time, which could result in convergent succession between warming and control. In contrast, the soil bacterial community is taxonomically, phylogenetically, and functionally highly diverse. They occupy heterogeneous niches, and could be subjected to multiple selection forces (e.g., resource limitation and intraspecific competition) 42 structuring community composition in response to climate warming, which could lead to the more dissimilar community over time.

Effects of warming on archaeal functional structure. The warming-altered archaeal taxonomic and phylogenetic composition could affect functional community structure. To test this, the microbial communities were further analyzed by both GeoChip-based functional gene arrays^{34, 44} and shotgun metagenomic sequencing. While the shotgun sequencing-based metagenomic approach is ideal for the novel discovery of phylotypes, functional genes, regulators, and/or metabolic pathways, the microarray-based detection has advantages for comparative studies in terms of sensitivity, quantitation, and reproducibility³⁴. Warming had significant (p < 0.001) impacts on the archaeal community functional structure (Adonis analysis, Table 1). Among the 188 archaea-specific genes detected by GeoChip, the abundances of 45 genes (23.9%) significantly decreased under warming (Supplementary Table S3). Some of these significantly impacted genes (16 out of 45 genes) were involved in C and N cycling (Fig. 1e, Supplementary Table S3). Among the 163 archaea-specific genes detected by metagenome

EcoFUN-MAP, warming had positive impacts on the abundances of eight genes and negative impacts on 16 genes, as shown by the response ratios (Supplementary Table S4). Four out of 24 genes significantly altered by warming were involved in C and N cycling (Fig. 1e, Supplementary Table S4). Two genes, aceB and ara, involved in C cycling were detected by both GeoChip and metagenome EcoFUN-MAP with significant differences between warming and control (Fig. 1e). However, the impacts of warming on these two genes by the two methods were opposite. It was most likely that the direction determined by GeoChip (decreased in abundance under warming) reflected the actual impact of warming as the results from amoA gene amplicon sequencing agreed with GeoChip data (Fig. 1e). In addition, four genes (ara, cda, xylanase, and amoA) from GeoChip but none from EcoFUN-MAP were strongly correlated with ecosystem C fluxes, including gross primary productivity (GPP) and ecosystem respiration (ER) (Supplementary Table S5 and S6). The ara, cda, and xylanase genes involve in C degradation processes, and amoA gene in nitrification. Collectively, these results indicate that warming significantly decreased the abundances of certain C and N cycling genes in the soil archaeal community but could strengthen the linkages between the archaeal functional community structure and ecosystem processes.

213

214

215

216

217

218

219

197

198

199

200

201

202

203

204

205

206

207

208

209

210

211

212

Community assembly processes in response to warming. To disentangle the community assembly mechanisms involved in the observed temporal succession patterns of soil archaeal community, we used a phylogenetic bin-based null model analysis (iCAMP)⁴⁵ and found that homogeneous selection (HoS; selection under homogeneous abiotic and biotic conditions in space and time) and drift (DR; random changes in the relative abundances of different species within a community due to the inherent stochastic processes of birth, death, and reproduction)

dominated archaeal community assembly, with the relative importance of 14.7% and 84.4% (Fig. 2a), respectively. Correspondingly, the partial canonical correlation analysis (CCA)-based variation partitioning analysis indicated that the majority of the community variations (86.4%) could not be explained by the measured soil and plant variables and time (Supplementary Fig. S5 and S6), suggesting that stochastic processes could play dominant roles in the assembly of soil archaeal community.

Over the years, the archaeal community variation between warming and control showed significant declines in stochasticity (Fig. 2b; slope = -0.015, p = 0.016) and DR (Fig. 2b; slope = -0.016, p = 0.028), but increase in HoS (Fig. 2b; slope = 0.015, p = 0.015), suggesting cumulatively enhanced deterministic filtering effect of warming on soil archaeal community. The increase in warming-induced determinism over time was significantly correlated with total plant biomass and total N (Fig. 2c, Supplementary Table S7; $|R| \ge 0.186$, $p \le 0.060$). Previous studies reported mixed effects of plant variables (richness and biomass) on deterministic assembly processes of soil bacterial communities 45, 46, but few on those of soil archaeal communities. Soil N content can be a determining factor for the fitness of AOA, the predominant group in soil archaeal communities⁴⁷.

The relative importance of different ecological processes varied substantially among different lineages (bins) (Fig. 3). The members of the predominating order Nitrososphaerales distributed in two bins, Bin2 (containing 23 OTUs, and accounting for 83.5% relative abundance) and Bin1 (46 OTUs, 15.1% relative abundance) (Fig. 3a, b). Unexpectedly, these two bins were dominated by different ecological processes — DR for Bin2 (99.8%) and HoS for Bin1 (97.2%).

Furthermore, the warming-induced decrease of DR was mainly due to Bin2 (69.1%, Fig. 3c and Extended Data Fig. 7), with OTU1 and OTU2 as the major contributors (contributed 24.3% and 26.1%, respectively; Supplementary Table S8). In contrast, the warming-induced increase of HoS was mainly attributed to the responses of Bin1 (98.6%, Fig. 3d and Extended Data Fig. 7), with OTU3 and OTU11 as top contributors (contributed 33.6% and 20.3%, respectively; Supplementary Table S8). Altogether, these results demonstrated complex assembly mechanisms of different taxa in response to warming, even within Nitrososphaerales.

250

251

252

253

254

255

256

257

258

259

260

261

262

263

264

265

243

244

245

246

247

248

249

Links between archaeal community structure and functioning. We compared correlations between archaeal community structure and environmental variables and ecosystem functioning under control and warming (Fig. 4a, Extended Data Fig. 8). The archaeal community measured by both taxonomical and gene functional compositions generally exhibited stronger correlations with various environmental variables and ecosystem functioning under warming than control (Fig. 4a, Extended Data Fig. 8). In fact, NH₄⁺-N, C₃ plant biomass, ER, and GPP were significantly correlated with archaeal community structure under warming (Fig. 4a, Extended Data Fig. 8; p < 0.05). Year was the most influential factor affecting archaeal community taxonomical and functional compositions under both warming and control, followed by total plant biomass. In addition, soil pH, precipitation of the sampling month, drought index, soil moisture, and ecosystem C fluxes including net ecosystem exchange (NEE) and heterotrophic soil respiration (R_h) were also factors significantly associated with archaeal community structure shared under warming and control (Fig. 4a, Extended Data Fig. 8; p < 0.05). Nevertheless, only a limited number of examined variables showed significant correlations with archaeal community taxonomical and functional structures under both warming and control.

266

267 Partial least squares (PLS) analysis was further used to understand the environmental drivers of 268 archaeal community diversity, succession, and associated functions under warming treatment 269 (Fig. 4b, Supplementary Table S9). Warming had a strong positive influence on soil temperature (Pearson correlation r = 0.92, partial $R^2 = 0.38$, p = 0.044) and to a lesser extent on soil pH (r =270 0.003, partial $R^2 = 0.17$, p = 0.015), but a negative influence on soil moisture (r = -0.50, partial 271 $R^2 = 0.22$, p = 0.007). Warming decreased archaeal community richness (r = -0.52, partial $R^2 =$ 272 0.21, p = 0.016), archaeal C degradation gene abundances (r = -0.57, partial $R^2 = 0.25$, p = 0.002) 273 and N functional gene abundances (r = -0.62, partial $R^2 = 0.20$, p = 0.001). In addition, warming 274 275 could shape archaeal community structure (i.e., β-diversity, PC2) indirectly through soil temperature (r = -0.03, partial R^2 = 0.23, p = 0.036) and archaeal community richness (r = -0.94, 276 partial $R^2 = 0.45$, p = 0.005). Soil total N (partial $R^2 \ge 0.24$, $p \le 0.005$) and archaeal functional 277 traits (i.e., nitrification and denitrification; partial $R^2 \ge 0.20$, $p \le 0.011$) also had strong effects on 278 279 archaeal β-diversity. Furthermore, the archaeal community functional traits involved in methane 280 and denitrification could positively impact ecosystem functions by affecting ER (partial $R^2 \ge$ 281 0.17, $p \le 0.006$). Lastly, the PLS model showed that soil properties such as soil total organic C, soil NH₄⁺-N, soil moisture, and soil temperature could directly shape ecosystem functions, 282 including autotrophic respiration (R_a), R_h, NEE, and ER (partial $R^2 \ge 0.34$, $p \le 0.006$). Together, 283 284 these results indicated that experimental warming could shape the soil archaeal community 285 directly or indirectly through soil temperature and that soil archaeal community structure was 286 crucial in mediating changes in ecosystem functioning.

287

288

Concluding remarks

Understanding temporal dynamics and its underlying mechanisms within the context of climate change is a fundamental issue in ecology; however, very few studies have examined the impacts of climate warming on Archaea. This study provides several important insights into the responses of the archaeal community to climate warming. First, consistent with our recent findings on the soil bacteria, fungi, and protists²⁷, we demonstrate that climate warming reduced the taxonomic, phylogenetic, and possibly functional diversity of soil archaeal community, which provides explicit evidence supporting microbial biodiversity loss under long-term climate warming in a field setting. Second, in contrast to the soil bacteria and fungi²⁵, we reveal that warming played an important role in accelerating the temporal succession of the soil archaeal community towards higher convergence, which could be primarily due to their distinct differences in biochemistry, physiology, ecology, and evolution⁸. In addition, our results demonstrated that the succession of soil archaeal community to the perturbations of climate warming was primarily controlled by stochastic processes, and experimental warming, acting as a filtering factor, reduced stochasticity.

Our findings have important implications for understanding and predicting the ecological consequences of climate change. Because stochasticity reduces under warming as time proceeds, the communities can converge more quickly to a community state with less stochasticity under warming. As a result, the archaeal community composition and structure might be less variable and more predictable under future climate warming. Also, since soil archaeal biodiversity decreases under warming, the future ecosystems in a warmer world will be less diverse. It is expected that the linked ecosystem functions and services could become more vulnerable under future climate warming scenarios³⁸. Consequently, the detrimental effects of biodiversity loss could be more severe. However, further research is needed to examine whether the warming-

- induced convergent succession, archaeal biodiversity loss, and associated mechanisms are
- 313 applicable to other ecosystems.

Acknowledgements

We thank all the former and current members of the Institute for Environmental Genomics for their time and energy in maintaining the long-term climate change experiment. This work is supported by the US Department of Energy, Office of Science, Genomic Science Program under Award Number DE-SC0004601 and DE-SC0010715, and the Office of the Vice President for Research at the University of Oklahoma. The data analysis performed by D.N. and N.X. was also partially supported by NSF Grants EF-2025558 and DEB-2129235.

Author contributions

All authors contributed intellectual input and assistance to this study. The original concepts were conceived by Y.Z. and J.Z. Field management was carried out by Y.Z., Linwei W., M.Y., X.Z., X.G., S.J., Z.Y., S.H., J.F., J.K., C.C., C.B., Y.F., J.M., Y.O., Y.F., D.N., Z.S., N.X., A.Z. and Liyou W. Sampling collection, soil chemical and microbial characterization were carried out by Y.H., M.Y., Linwei W., J.G., and Z.G. Data analyses were done by Y.Z. and D.N. with the assistance provided by Linwei W., and J.Z. All data analysis and integration were guided by J.Z.

The manuscript was prepared by Y.Z., D.N., X.L., Y.Y., J.T., and J.Z.

Competing interests

332 The authors declare no competing interests.

Table 1. Summary of permutational multivariate analysis of warming, year, block on soil archaea community structure.

334

335 336

fabricate GeoChip.

Variables	16S rRNA gene			GeoChip			Metagenome EcoFUN-MAP		
	\overline{F}	R^2	p	\overline{F}	R^2	p	\overline{F}	R^2	p
Warming (W)	3.923	0.040	0.014	6.037	0.047	0.001	2.215	0.031	0.001
Year (Y)	3.877	0.274	0.001	8.857	0.485	0.001	1.922	0.189	0.001
Block (B)	2.277	0.069	0.026	1.847	0.043	0.031	1.194	0.050	0.071
Y*B	1.437	0.305	0.066	1.113	0.183	0.278	1.002	0.295	0.443

337 338 Permutational multivariate analysis of variance (Adonis) was used based on Bray-Curtis dissimilarity 339 matrices. The two-way repeated measures ANOVA model was set as dissimilarity ~ warming + year × block 340 using function adonis in R package vegan. Significant effects (p < 0.05) are shown in bold text. EcoFUN-MAP 341 is a method designed for annotating metagenomic sequences by comparing them with functional genes used to 342

Figure Legends

344

343

345

346

347

348

349

350

351

352

353

354

355

356

357

358

359

360

361

362

363

364

365

366

367

368

369

370

371

372

Fig. 1. Effects of experimental warming on the archaeal community diversity and succession across seven years. a, Archaeal community composition under unwarmed and warmed conditions. Cumulative richness is expressed as the number of operational taxonomic units (OTUs). b, The effect sizes of warming on archaeal biodiversity (including taxonomic, phylogenetic, and functional diversity). The estimated effect sizes (β) are regression coefficients based on rescaled response variables (rescaled to one with mean zero and unit standard deviation) in the linear mixed-effects (LMMs) models. Bars represent mean \pm s.e.m. of effect sizes. Statistical significance is based on Wald type II γ^2 tests (n = 64; two-sided; p = 0.008, 0.006, 0.070, 0.533 for 16S richness, 16S PD, GeoChip richness, and EcoFUN-MAP richness, respectively). Significance was expressed as ***p < 0.01; **p < 0.05; *p < 0.10. EcoFUN-MAP is a method designed for annotating metagenomic sequences by comparing them with functional genes used to fabricate GeoChip. c and d, Temporal changes in community differences between warming and control conditions. c, 16S rRNA genes (left: Sorensen dissimilarity metrics; right: unweighted UniFrac dissimilarity metrics); **d**, amoA genes. The slopes of the archaeal community and the bacterial community are significantly different in c (p = 0.007 and p < 0.0070.001). The first year is 2009 (year 0). Considering the repeated-measures design, the warmingversus-control dissimilarity values at each block were fitted to LMMs with a fixed effect of time and a random intercept and slope effect among different pairs of plots (blocks). The slopes are presented as a coefficient in fixed effect \pm standard error in random effect. The r^2 values are calculated (details in Methods) to reflect the variance explained by the whole LMM model. p values were based on permutation tests (two-sided). The lines showed the fixed effects of the LMM. e, Differences in functional gene abundances between warming and control by response ratios. Bars represent mean \pm 95% confidence interval of response ratios. Only genes showing significant differences between warming and control (p < 0.05, n = 64) are shown. EFM: metagenome EcoFUN-MAP; A: amoA genes (mean relative abundance > 10.0%).

Fig. 2. Ecological processes and community assembly mechanisms associated with the temporal dynamics in the soil archaeal community. a, Relative importance of deterministic processes (homogeneous selection, HoS; heterogeneous selection, HeS) and stochastic processes (dispersal limitation, DL; homogenizing dispersal, HD; and drift and others, DR) between warming and control treatment. b, Changes in the relative importance of stochastic processes, HoS, and DR (%) between warming and control at each block over the years. Results are based on LMMs (statistical tests and significance are the same as in Fig. 1c-d). c, Effects of environmental factors on deterministic processes defined by the phylogenetic bin-based null model analysis (iCAMP) based on the Mantel test (two-sided). It only shows the factors with significant correlations (p = 0.039, 0.062, 0.049, 0.029 for total N, total organic C, total plant biomass, and the difference of plant richness). See Supplementary Table S7 for other factors. R, coefficient of determination from the Mantel analysis. The correlation was determined based on the difference (with a triangle before the name) or the mean (without a triangle) of a factor between each pair of samples. Significance was expressed as ***p < 0.01; **p < 0.05; *p < 0.10.

Fig. 3. Variations of ecological processes across different phylogenetic groups. The phylogenetic tree is displayed at the center. **a**, Relative importance of different ecological processes in each bin (stacked bars in the 1st annulus). **b**, Relative abundance of individual taxonomic units (2nd annulus). All 287 taxonomic units are shown. **c**, Warming-induced change in taxonomic unit contribution to drift (3rd annulus), and **d**, homogeneous selection (4th annulus), where positive (outward bar) and negative (inward bar) represented increase and decrease by warming, respectively. The most abundant bins are marked in the figure, including Bin2 (83.5% relative abundance; dominated by Nitrososphaerales), Bin1 (15.1%; Nitrososphaerales), Bin4 (0.9%; Methanomassiliicoccales) and Bin3 (0.2%; unclassified Euryarchaeota).

Fig. 4. Environmental drivers of archaeal community structure and functioning. a, Relationships between archaeal community structure and environmental variables and ecosystem processes under warming. See Supplementary Fig. S8 for under control. Archaeal community structures, which include taxonomical composition by 16S rRNA genes and functional gene

404 composition by GeoChip and EcoFUN-MAP, were tested against time, soil and plant variables, 405 and ecosystem C fluxes. The edge width corresponds to Mantel's r value, and the edge color 406 denotes statistical significance (two-sided). Pairwise correlations of these variables are shown 407 with a color gradient denoting Pearson's correlation coefficient. Soil variables include soil nitrate 408 (NO₃⁻), ammonium (NH₄⁺), total nitrogen (TN), total organic C (TOC), pH, precipitation of the 409 sampling month (Prcp SM), temperature, moisture, and drought index; plant variables include 410 C₃ and C₄ aboveground biomass, plant richness, and total biomass; ecosystem C fluxes include 411 ecosystem respiration (ER), gross primary productivity (GPP), net ecosystem exchange (NEE), 412 autotrophic respiration (R_a), heterotrophic respiration (R_h), and total soil respiration (R_t). **b**, Partial least squares (PLS) models on the relationships among treatments (warming), soil 413 414 properties, plant variables, archaeal community diversity and functional traits, and ecosystem functions. Directions for all arrows are from independent variable(s) to a dependent variable in 415 the forward selected PLS models (p < 0.05 for both R^2_y and Q^2_y ; two-sided); only the most 416 417 relevant variables (variable influence on projection > 1) are presented. The numbers near the 418 pathway arrow indicate the proportion of variance explained for every dependent variable, with the top row representing the partial R² index based on PLS (See details in Methods) and the 419 bottom row representing Pearson correlation R². The asterisks denote the significance levels of 420 each optimum PLS model (top row) and Pearson correlation (bottom row). ***p < 0.01, **p < 0.01421 0.05 and *p < 0.10. The widths of pathways are proportional to the partial R^2 index. 422

423424

425

References

- Woese, C.R., Kandler, O. & Wheelis, M.L. Towards a natural system of organisms:
 proposal for the domains Archaea, Bacteria, and Eucarya. *Proc Natl Acad Sci USA* 87,
 428
 4576-4579 (1990).
- 429 2. Hedlund, B.P., Zhang, C., Wang, F., Rinke, C. & Martin, W.F. Editorial: Ecology,
 430 Metabolism and Evolution of Archaea-Perspectives From Proceedings of the
- International Workshop on Geo-Omics of Archaea. *Front Microbiol* **12**, 827229 (2021).
- 432 3. DeLong, E.F. Archaea in coastal marine environments. *Proc Natl Acad Sci USA* **89**, 433 5685-5689 (1992).
- 434 4. Fuhrman, J.A., McCallum, K. & Davis, A.A. Novel major archaebacterial group from marine plankton. *Nature* **356**, 148-149 (1992).
- DeLong, E.F. Exploring Marine Planktonic Archaea: Then and Now. Front Microbiol 11
 (2021).

- 438 6. Karimi, B. et al. Biogeography of soil bacteria and archaea across France. *Sci Adv* **4** 439 (2018).
- Tahon, G., Geesink, P. & Ettema, T.J.G. Expanding Archaeal Diversity and Phylogeny: Past, Present, and Future. *Annu Rev Microbiol* **75**, 359-381 (2021).
- 8. Baker, B.J. et al. Diversity, ecology and evolution of Archaea. *Nat Microbiol* **5**, 887-900 (2020).
- 9. Needham, D.M. & Fuhrman, J.A. Pronounced daily succession of phytoplankton, archaea and bacteria following a spring bloom. *Nat Microbiol* **1**, 16005 (2016).
- 446 10. Shu, W.S. & Huang, L.N. Microbial diversity in extreme environments. *Nat Rev Microbiol* (2021).
- 448 11. Adam, P.S., Borrel, G., Brochier-Armanet, C. & Gribaldo, S. The growing tree of 449 Archaea: new perspectives on their diversity, evolution and ecology. *ISME J* 11, 2407-450 2425 (2017).
- 451 12. Zaremba-Niedzwiedzka, K. et al. Asgard archaea illuminate the origin of eukaryotic cellular complexity. *Nature* **541**, 353-358 (2017).
- Imachi, H. et al. Isolation of an archaeon at the prokaryote-eukaryote interface. *Nature* 577, 519-525 (2020).
- Liu, Y. et al. Expanded diversity of Asgard archaea and their relationships with eukaryotes. *Nature* (2021).
- 457 15. Angel, R., Soares, M.I., Ungar, E.D. & Gillor, O. Biogeography of soil archaea and bacteria along a steep precipitation gradient. *ISME J* **4**, 553-563 (2010).
- 459 16. Auguet, J.C., Barberan, A. & Casamayor, E.O. Global ecological patterns in uncultured 460 Archaea. *ISME J* **4**, 182-190 (2010).
- Hates, S.T. et al. Examining the global distribution of dominant archaeal populations in soil. *ISME J* **5**, 908-917 (2011).
- Har-On, Y.M., Phillips, R. & Milo, R. The biomass distribution on Earth. *Proc Natl Acad Sci USA* **115**, 6506-6511 (2018).
- 465 19. Offre, P., Spang, A. & Schleper, C. Archaea in Biogeochemical Cycles. *Annu Rev Microbiol* 67, 437-457 (2013).
- 467 20. Leininger, S. et al. Archaea predominate among ammonia-oxidizing prokaryotes in soils. *Nature* **442**, 806-809 (2006).
- Danovaro, R., Rastelli, E., Corinaldesi, C., Tangherlini, M. & Dell'Anno, A. Marine archaea and archaeal viruses under global change. *F1000Res* **6**, 1241 (2017).
- 471 22. Goberna, M., Garcia, C., Insam, H., Hernandez, M.T. & Verdu, M. Burning fire-prone 472 Mediterranean shrublands: immediate changes in soil microbial community structure and 473 ecosystem functions. *Microb Ecol* **64**, 242-255 (2012).
- Gschwendtner, S. et al. Climate change induces shifts in abundance and activity pattern of bacteria and archaea catalyzing major transformation steps in nitrogen turnover in a soil from a mid-European beech forest. *PLoS One* **9**, e114278 (2014).
- Hayden, H.L. et al. Changes in the microbial community structure of bacteria, archaea and fungi in response to elevated CO(2) and warming in an Australian native grassland soil. *Environ Microbiol* **14**, 3081-3096 (2012).
- 480 25. Guo, X. et al. Climate warming leads to divergent succession of grassland microbial communities. *Nat Clim Change* **8**, 813-818 (2018).
- 482 26. Guo, X. et al. Climate warming accelerates temporal scaling of grassland soil microbial biodiversity. *Nat Ecol Evol* **3**, 612-619 (2019).

- Wu, L. et al. Reduction of microbial diversity in grassland soil is driven by long-term climate warming. *Nat Microbiol* **7**, 1054-1062 (2022).
- 486 28. Yuan, M.M. et al. Climate warming enhances microbial network complexity and stability. *Nat Clim Change* (2021).
- 488 29. Cavicchioli, R. Archaea--timeline of the third domain. *Nat Rev Microbiol* **9**, 51-61 (2011).
- 490 30. Prach, K. & Walker, L.R. Four opportunities for studies of ecological succession. *Trends Ecol Evol* **26**, 119-123 (2011).
- 492 31. Xu, X., Sherry, R.A., Niu, S.L., Li, D.J. & Luo, Y.Q. Net primary productivity and rain-493 use efficiency as affected by warming, altered precipitation, and clipping in a mixed-494 grass prairie. *Global Change Biol* **19**, 2753-2764 (2013).
- 495 32. Kerou, M., Alves, R.J.E. & Schleper, C. N itrososphaerales. *Bergey's Manual of Systematics of Archaea and Bacteria*, 1-4 (2015).
- 497 33. Nkamga, V.D. & Drancourt, M. Methanomassiliicoccales. *Bergey's Manual of Systematics of Archaea and Bacteria*, 1-2 (2015).
- Zhou, J. et al. High-throughput metagenomic technologies for complex microbial community analysis: open and closed formats. *mBio* **6** (2015).
- 501 35. Zhou, J. et al. Random sampling process leads to overestimation of beta-diversity of microbial communities. *mBio* 4, e00324-00313 (2013).
- 36. Xue, K. et al. Tundra soil carbon is vulnerable to rapid microbial decomposition under climate warming. *Nat Clim Change* **6**, 595-600 (2016).
- 505 37. Pecl, G.T. et al. Biodiversity redistribution under climate change: Impacts on ecosystems and human well-being. *Science* **355** (2017).
- 507 38. Cardinale, B.J. et al. Biodiversity loss and its impact on humanity. *Nature* **486**, 59-67 (2012).
- 509 39. Li, D., Miller, J.E.D. & Harrison, S. Climate drives loss of phylogenetic diversity in a grassland community. *Proc Natl Acad Sci USA* **116**, 19989-19994 (2019).
- Fei, S. et al. Divergence of species responses to climate change. *Sci Adv* **3**, e1603055 (2017).
- 513 41. Bascompte, J., García, M.B., Ortega, R., Rezende, E.L. & Pironon, S. Mutualistic interactions reshuffle the effects of climate change on plants across the tree of life. *Sci Adv* 5, eaav2539 (2019).
- 516 42. Kerou, M. et al. Proteomics and comparative genomics of Nitrososphaera viennensis 517 reveal the core genome and adaptations of archaeal ammonia oxidizers. *Proc Natl Acad* 518 *Sci USA* **113**, E7937-E7946 (2016).
- Taylor, A.E., Giguere, A.T., Zoebelein, C.M., Myrold, D.D. & Bottomley, P.J. Modeling of soil nitrification responses to temperature reveals thermodynamic differences between ammonia-oxidizing activity of archaea and bacteria. *ISME J* 11, 896-908 (2017).
- 522 44. Shi, Z. et al. Functional Gene Array-Based Ultrasensitive and Quantitative Detection of Microbial Populations in Complex Communities. *mSystems* 4 (2019).
- Ning, D.L. et al. A quantitative framework reveals ecological drivers of grassland microbial community assembly in response to warming. *Nat Commun* **11** (2020).
- 526 46. Liu, L. et al. Changes in assembly processes of soil microbial communities during secondary succession in two subtropical forests. *Soil Biol Biochem* **154**, 108144 (2021).

Verhamme, D.T., Prosser, J.I. & Nicol, G.W. Ammonia concentration determines
 differential growth of ammonia-oxidising archaea and bacteria in soil microcosms. *ISME* J5, 1067-1071 (2011).

Methods:

532

533

534

535

536

537

538

539

540

541

542

543

544

545

546

547

548

549

550

551

552

553

554

Site description. The study site was located at the Kessler Atmospheric and Ecological Field Station (KAEFS) in the US Great Plains in McClain County, Oklahoma (34°59′ N, 97°31′ W)³¹. The design of this site has been described in detail in our previous publications^{25, 28, 48}. Briefly, KAEFS is a temperate grassland with an average air temperature of 16.3 °C and an average annual precipitation of 914 mm (data from the Oklahoma Climatological Survey from 1948 to 1999). The experimental site was dominated by C₃ forbs (Solanum carolinense, Ambrosia trifida and Euphorbia dentate), C₃ grasses (Bromus sps) and C₄ grasses (Tridens flavus and Sorghum halapense). The soil type was Port-Pulaski-Keokuk complex, with a neutral pH, a high available water holding capacity (37%) and a deep (ca. 70 cm), moderately penetrable root zone²⁵. The soil has a high available water holding capacity (37%), neutral pH, and a deep (ca. 70 cm), moderately penetrable root zone. The concentrations of soil organic matter and total N are 1.9% and 0.1%, respectively, and the soil bulk density is 1.2 g/cm³. The field experiment started in July 2009 and is a split-block design, with warming (+3 °C) as the primary factor. Two levels of warming (ambient and $+3^{\circ}$ C) were set for four pairs of 2.5 m \times 1.75 m plots by utilizing a 'real' infrared radiator (Kalglo Electronics) for warmed plots or a 'dummy' infrared radiator (Kalglo Electronics) for the corresponding control plots to account for the shading effects. In this study, data generated from this site between 2009 and 2016 was used. **Field measurements.** Soil temperature was monitored using constantan-copper thermocouples

every 15 min at 7.5, 20, 45 and 75 cm in the center of each plot. We used the annual average

values at 7.5 cm depth across the whole year to represent the microclimate of the surface soil

sampled (0-15 cm). Soil moisture, expressed as volumetric soil water content (%V), was measured once or twice a month using a portable time domain reflectometer (Soil Moisture Equipment Corp.) from the soil surface to a 15-cm depth. The average values of three measurements in each plot were used as monthly averages and the average of soil moisture data across each year was presented in this study. All species within each plot were identified to estimate species richness. Above-ground plant biomass was estimated by a modified pin-touch method^{31, 49} with C₃ and C₄ species separated⁵⁰.

Ecosystem C fluxes, including NEE, ER, GPP, soil total respiration (R_t), R_h , and R_a were measured once or twice a month between 10:00 and 15:00 (local time)^{31, 51}. NEE and ER were measured using an LI-6400 portable photosynthesis system (LI-COR) attached to a transparent chamber (0.5 m × 0.5 m × 0.7 m). R_t and R_h were measured using an LI-8100A soil flux system attached to a soil CO₂ flux chamber (LI-COR)⁵². GPP was estimated as the difference between NEE and ER and R_a was the difference between R_t and R_h . The average values of ecosystem C fluxes and respirations across each year were used in this study.

Sampling. We collected eight surface (0-15 cm) soil samples annually in four control and four warmed plots from 2010 to 2016 (Y1-Y7) during the peak plant biomass season (September to October). Eight pre-warmed samples were taken in 2009 (Y0). Each soil sample was a mixture of three soil cores (2.5 cm diameter × 15 cm depth) taken with a soil sampler tube to reduce the variation caused by soil heterogeneity. A total of 64 soil samples from four replicate plots under warming and control (ambient) conditions were included and analyzed in this study. Soil samples

were kept on ice for less than two hours before they were transferred to the laboratory located at the University of Oklahoma.

Soil chemistry. After removing visible roots (> 0.25 cm) and rocks, soil samples were sent to the Soil, Water, and Forage Analytical Laboratory at the Oklahoma State University (Stillwater, OK, USA) for chemical analyses, including organic C and total N contents, soil nitrate (NO₃⁻) and ammonia (NH₄⁺), and soil pH. Detailed information was provided in our previous publication by Guo *et al.*²⁵. As shown previously, experimental warming significantly altered aboveground plants, ecosystem processes, and soil conditions^{25, 48}. For microbiological analyses, samples were stored at -80 °C before DNA extraction.

DNA extraction. Soil DNA was extracted from 1.5g of each well-mixed soil sample by a protocol^{25, 53} including freeze-grinding treatment, SDS-based lysis, followed by purification with a MoBio PowerSoil DNA isolation kit (MoBio Laboratories, Carlsbad, CA, USA). DNA quality was assessed with a NanoDrop ND-1000 Spectrophotometer (Thermo Fisher Scientific, Waltham, MA, USA) and a ratio of 2.0-2.2 for OD260/OD230 and 1.7-2.0 for OD260/OD280 indicated good quality. The final DNA concentrations were quantified by PicoGreen using a FLUOstar Optima fluorescence plant reader (BMG Labtech, Orthenberg, Germany). DNAs were stored at -80 °C before sequencing analysis²⁵.

Amplicon sequencing. We used a two-step PCR amplification protocol for constructing the sequencing library to reduce sequencing errors, minimize amplification bias, and preserve semi-quantitative information of PCR amplification^{36, 54, 55}. In this study, we used one primer set

targeting the V3–V4 hypervariable region of the archaeal 16S rRNA genes, 519F (5' -CAGYMGCCRCGGKAAHACC -3') and 806R (5' - GGACTACNSGGGTMTCTAAT -3')⁵⁶⁻⁵⁸. To amplify the archaeal *amoA* genes, the primer set (5'-STAATGGTCTGGCTTAGACG-3') and (5'-GCGGCCATCCATCTGTATGT-3')⁵⁹ was used. In addition, the primer set, 515F (5'-GTGCCAGCMGCCGCGGTAA-3') and 806R (5'-GGACTACHVGGGTWTCTAAT-3'), were used for bacterial community profiling⁶⁰. During the first amplification step, 10 ng DNA from each sample was PCR-amplified for 10 cycles in a 25 µl reaction volume with the primers without adaptors. The obtained PCR products were then purified and dissolved in 50 µl deionized water. During the second amplification step, 15 µl of the PCR products from each sample were amplified using the primers with adaptors, barcodes, and spacers for an additional 15 cycles. The PCR reactions at each step were done in triplicates. Paired-end sequencing of the amplicons (2 × 250 bp) was done with an Illumina MiSeq platform (Illumina, Inc., San Diego, CA, USA) following manufacturer's instructions for both the archaeal and bacterial 16S rRNA genes^{54, 55}. For sequencing the archaeal *amoA* gene amplicons, MiSeq Reagent Kit v3 (2×300 bp) (Illumina, Inc., San Diego, CA, USA) was used. An average of $29,900 \pm 20,800, 25296 \pm 100$ 20560, and $59900 \pm 36{,}700$ sequence reads per sample were obtained for the archaeal 16S rRNA genes, archaeal amoA genes, and bacterial 16S rRNA genes, respectively. **Sequence preprocessing.** The raw reads of sequences were analyzed using a sequence analysis pipeline built on the Galaxy platform (version 0.1.0), developed by the Institute for Environmental Genomics⁶¹ (http://zhoulab5.rccc.ou.edu:8080). Primer sequences were trimmed from the paired-end sequences and filtered by the Btrim program⁶² with a threshold of QC > 20over a 5-bp window size. Forward and reverse reads of the same sequence with at least 20 bp

600

601

602

603

604

605

606

607

608

609

610

611

612

613

614

615

616

617

618

619

620

621

overlap and < 5% mismatches were combined using FLASH⁶³. Any joined sequences with an ambiguous base or a length of < 245 bp were discarded. Because the expected lengths of the archaeal amoA gene amplicons (635 bp) were larger than the summed length of forward and reverse reads (600 bp), we only used the forward reads of the archaeal amoA gene amplicons with a cutoff length of 273 nt. Thereafter, OTUs were clustered by UPARSE⁶⁴ at 97% identity and singletons were removed from the remaining sequences^{64, 65}. The Greengenes reference data set⁶⁶ for 16S data was used as reference databases to remove chimeras. For the archaeal community, each sample was rarefied to a sequencing depth of 7,860 to achieve the same total read abundance. A total of 287 OTUs (at 97% similarity) were obtained across all samples. Rarefaction curves approached saturation, suggesting that this level of sequencing effort was sufficient to estimate the diversity of the soil archaeal community (Extended Data Fig. 9). In comparison, the bacterial community was rarefied to a sequencing depth of 21,200 with 35,306 OTUs across all samples. OTU taxonomic classification was performed using representative sequences from each OTU through the Ribosomal Database Project Classifier with 50% confidence estimates⁶⁷. We also constructed community profiling based on amplicon sequence variants (ASVs) by three widely-used denoising packages UNOISE3⁶⁸, DADA2⁶⁹, and Deblur⁷⁰. We compared the effects of experimental warming on the resulting community profiles by three non-parametric multivariate statistical tests (Adonis, ANOSIM, and MRPP; Supplementary Table S2). OTU-based archaeal community structure was significantly altered by seven years' warming treatment with all three statistical tests (p < 0.050), while UNOISE3, DADA2, and Deblur community profiles showed significant (p < 0.050) or marginally significant (p < 0.100) differences by warming treatment in some of the tests but not all (Supplementary Table S1). It suggested that the community structure obtained from OTU-based clustering was more robust to

623

624

625

626

627

628

629

630

631

632

633

634

635

636

637

638

639

640

641

642

643

644

different statistical tests and agreed with the experimental setup. Therefore, the community profiling obtained from OTU-based clustering was used in the following analyses.

Diversity analyses. Richness and Faith's index were used to measure taxonomic and phylogenetic α-diversity, respectively, and they were computed using the *Picante* R package⁷¹. To estimate phylogenetic β-diversity, the representative amplicon sequences were aligned using Clustal Omega v1.2.2⁷² for constructing the phylogenetic tree by FastTree2 v2.1.10⁷³. The FastTree topology search was constrained with the relatively reliable 16S-based phylogenetic tree in Silva Living Tree Project⁷⁴ release 132. Unweighted UniFrac distances and Sorensen dissimilarity metrics were calculated to estimate β-diversity based on the resampled OTU tables in R using the *vegan* package⁷⁵.

Measurement of community turnover. The impacts of warming on the temporal change in the archaeal and bacterial community structure were measured by the distances of microbial communities between warming and control at each block in each year⁷⁶. As we had four replicates (one replicate within each block) for both warming and control treatments, four pairwise comparisons were obtained each year. In this way, the difference between each pair of plots (D) was not subject to (in theory) the effects of experimental noise due to annual sampling time differences, environmental fluctuations, molecular marker resolution, and/or technical variation on community temporal turnovers. We then fitted the temporal change to the linear mixed effects model (LMM) with a random intercept and sloped effect among different pairs of plots (blocks)²⁵, D ~ t + (1 + t)|Block. In this model, D represents dissimilarity between warming and control and t represents year. The slope of the model is the rate of temporal change in

community structure between warming and control, which is a measure of community turnover. The coefficient of determination (R^2) was calculated for each LMM as described previously (named conditional R^2 in Nakagawa and Schielzeth's method)⁷⁷. The significance of each LMM was calculated by a permutation test, randomized the eight time points (years) for > 40,000 times (complete enumeration), and the p value was calculated by comparing the Akaike information criterion of the observed LMM with the permuted ones. We also performed a permutation test to calculate the significance of the difference in slopes between warming and control ⁷⁸. The p-value was generated by comparing the observed slope difference between warming and control with the difference in the permuted data sets²⁵.

Functional profiling. GeoChip 5.0 M, a functional gene array³⁴, was used for functional profiling for the 64 samples from 2009 to 2016. GeoChip hybridization, scanning, and data processing were performed in the Institute for Environmental Genomics, the University of Oklahoma, following an established protocol^{34, 44}.

The slides hybridized with genomic DNA were imaged as a Multi-TIFF with a NimbleGen MS200 Microarray Scanner (Roche NimbleGen, Madison, WI, United States). The raw signals from NimbleGen were submitted to the Microarray Data Manager (http://ieg.ou.edu/microarray), cleaned, normalized, and analyzed using the data analysis pipeline. First, probes with poor or low signals were removed using a cutoff for the coefficient of variance (CV; probe signal SD/signal) >0.8. Then, the signal-to-noise ratio (SNR) was calculated with the average signal of Agilent's negative control probes within each subarray. The signal intensity for each spot was corrected by subtracting the background signal intensity. If the net difference was <0, the spots

were excluded from subsequent analysis⁴⁴. To normalize signal intensities, the sum of the signal intensity was calculated for each array, and the maximum sum value was used to normalize the signal intensity of all spots in each array. We extracted 2524 archaea-specific probes from the entire datasets based on their lineage information, which belonged to 188 archaea-specific genes. All the analyses were done using the extracted subset of data.

697

698

699

700

701

702

703

704

705

706

707

708

709

710

711

712

692

693

694

695

696

Metagenomics of individual samples from 2009 to 2016 was also used for functional profiling. Metagenomic libraries were prepared using a KAPA Hyper Prep Kit (KR0961) following the manufacturer's instructions and sequenced at the Oklahoma Medical Research Foundation's Genomics Core using the Illumina HiSeq 3000 platform with a 2 × 150 bp paired-end kit. We obtained 1100.14 gigabases (Gb) of data in total, with an average of 17.19 \pm 2.68 Gb per sample²⁷. Processing of the metagenomic sequences included quality evaluation by FastQC⁷⁹, duplicate removal by CD-HIT⁸⁰ with an identity cutoff of 100%, and quality filtering by NGS QC Toolkit (version 2.3.3)81. Bases with a quality score <20 were trimmed from the 3' end until the first base had a quality score ≥ 20 . Trimmed reads with a length of > 120 and an average quality score ≥ 20 were kept. In addition, reads with more than one ambiguous base were removed²⁷. All reads were submitted to our EcoFUN-MAP pipeline (http://www.ou.edu/ieg/tools/dataanalysis-pipeline.html) to extract shotgun sequence reads of environmental importance³⁶. Archaea-specific gene clusters were extracted from the entire datasets based on their lineage information, resulting in 21031 gene clusters belonging to 163 genes. This archaea-specific dataset was used in the following analyses.

Community assembly. The iCAMP framework was used to investigate the community assembly mechanisms at the level of individual taxa/lineages⁴⁵. The R code for iCAMP was available as an open-source R package, iCAMP, and a web-based pipeline (http://ieg3.rccc.ou.edu:8080) built on the Galaxy platform (version 18.09)⁶¹. iCAMP could differentiate the relative importance of five assembly processes to both the whole community and individual taxa/lineages, including homogeneous selection (HoS), heterogeneous selection (HeS), dispersal limitation (DL), homogenizing dispersal (HD), and drift and others (DR)^{45, 82}. Defined in iCAMP, HoS and HeS constituted deterministic processes, while DL, HD, and DR constituted stochastic processes. Our analyses were based on a phylogenetic distance threshold for the significant phylogenetic signal of 0.2 and a minimal bin size of 12. Detailed explanations of the settings for individual parameters could be found in a previous study⁴⁵. The five assembly processes were assessed for their relative importance in governing community variations between warmed plots and control plots. Then, the relative importance of each process was fitted to an LMM with a random intercept and slope effect among different pairs of plots (blocks). The model was set as $M \sim t + (1 + t)|Block$, where M represents the relative importance (%) of a process and t represents year. The coefficient of determination (R²) and the significance of each LMM was determined as described above. **Statistical analyses.** Statistical analyses were carried out using R software 4.0.2 with the

714

715

716

717

718

719

720

721

722

723

724

725

726

727

728

729

730

731

732

733

734

735

736

Statistical analyses. Statistical analyses were carried out using R software 4.0.2 with the package *vegan* (v.2.5-7) unless otherwise indicated. Three different non-parametric multivariate statistical tests (Adonis, ANOSIM, and MRPP) were used to test the differences in soil microbial communities under warming and control treatments⁵¹. For Adonis, the one-way repeated-measures ANOVA model was set as 'dissimilarity ~ warming + block × year' when using the

function Adonis in the R package *vegan*. For ANOSIM and MRPP, the permutation was constrained within each block in each year by setting 'strata' in the functions ANOSIM and MRPP in the R package *vegan*²⁵. CCA was performed to determine the linkage between ecosystem functional parameters and microbial community structures. The significance of the CCA model was tested using ANOVA. Based on CCA results, variation partitioning analysis was performed to determine the contributions of each variable or group of variables to total variations in the soil microbial community composition. Mantel and partial Mantel tests were also performed to calculate the correlations between environmental factors and soil microbial communities.

The PLS model was used to explore the relationships among treatments (warming), archaea community diversity, plant variables, and soil properties 83 . Each optimum PLS model is forward selected from all factors which may affect the dependent variable in biology/biogeochemistry, based on predictive performance counting in the explained variation (R2Y) and model significance (p for R^2_Y and $Q^2_Y < 0.05$, where significant Q^2_Y helps to avoid overfitting). To visualize relevant associations, we only include the most relevant variable(s) with Variable Influence on Projection (VIP) values higher than 1.00^{83} . When used as independent variables in PLS, the archaeal community beta-diversity was represented by the PC1-3 from Principal Coordinates Analysis of Sorensen distance. Inspired by VIP, we proposed a partial R^2 index based on PLS to represent the proportion of variance explained by each independent variable (Eq.1). As a reference, we also calculated the pairwise correlation coefficient (as well as the R^2) among the factors and the significance is based on Pearson correlation (between vectors) or Mantel test (between distance matrixes). The PLS-related analysis was performed using the *ropls*

package in R⁸⁴, and the Mantel test by the *vegan* package⁷⁵. A list of potential predictors
 (independent variables, X) for each factor (dependent variable, Y) tested by PLS was included in
 Supplementary Table S9.

$$R_{PLSj}^2 = R_Y^2 \times \frac{\Sigma_f \left(W_{jf}^2 \times SSY_f \right)}{SSY_{cum}} = \frac{\Sigma_f \left(W_{jf}^2 \times SSY_f \right)}{SSY} \quad (Eq.1)$$

- $R_{PLS_i}^2$ Partial R^2 of variable j based on PLS.
- 767 W_{if} The PLS weight of variable j on component f.
- 768 SSY_f The sum of squares of Y explained by component f.
- 769 SSY_{cum}The cumulative sum of squares of Y explained by all components.
- R_Y^2 The percentage of Y dispersion (i.e., sum of squares) explained by the PLS model.
- 771 SSY Y dispersion, i.e., sum of squares of Y.

Data availability

The DNA sequences of the archaeal 16S rRNA gene amplicons are available in the National Center for Biotechnology Information (NCBI) Sequence Read Archive under project accession number PRJNA861672. The DNA sequences of the bacterial 16S rRNA gene amplicons were under the project accession number PRJNA331185. Raw shotgun metagenomic sequences are deposited in the European Nucleotide Archive (http://www.ebi.ac.uk/ena) under study no. PRJNA533082. The soil physical and chemical attributes, and plant biomass and richness are downloadable online at http://www.ou.edu/ieg/publications/datasets. Silva 132 Ref NR database is available at https://www.arb-silva.de/documentation/release-132/. Greengene reference data set is available from the QIIME GitHub repository https://github.com/biocore/qiime-default-reference/gg_13_8_otus/rep_set/97_otus.fasta.gz. Source data are provided with this paper.

787 Code availability

- 788 R scripts for statistical analyses are available on GitHub at
- 789 https://github.com/yazhang2022/OKwarmingsiteArchaea.

790

791

792

References

- Guo, X. et al. Gene-informed decomposition model predicts lower soil carbon loss due to persistent microbial adaptation to warming. *Nat Commun* **11** (2020).
- Frank, D.A. & McNaughton, S.J. Aboveground biomass estimation with the canopy intercept method: a plant growth form caveat. *Oikos*, 57-60 (1990).
- 50. Sherry, R.A. et al. Lagged effects of experimental warming and doubled precipitation on annual and seasonal aboveground biomass production in a tallgrass prairie. *Global Change Biol* 14, 2923-2936 (2008).
- 800 51. Zhou, J.Z. et al. Microbial mediation of carbon-cycle feedbacks to climate warming. *Nat Clim Change* **2**, 106-110 (2012).
- Li, D., Zhou, X., Wu, L., Zhou, J. & Luo, Y. Contrasting responses of heterotrophic and autotrophic respiration to experimental warming in a winter annual-dominated prairie.

 Global Change Biol 19, 3553-3564 (2013).
- Zhou, J., Bruns, M.A. & Tiedje, J.M. DNA recovery from soils of diverse composition. Appl. Environ. Microbiol. **62**, 316-322 (1996).
- Wu, L. et al. Phasing amplicon sequencing on Illumina Miseq for robust environmental microbial community analysis. *BMC Microbiol* **15**, 125 (2015).
- Solution Science Scien
- Suzuki, M.T. & Giovannoni, S.J. Bias caused by template annealing in the amplification of mixtures of 16S rRNA genes by PCR. *Appl Environ Microbiol* **62**, 625-630 (1996).
- Takai, K. & Horikoshi, K. Rapid detection and quantification of members of the archaeal community by quantitative PCR using fluorogenic probes. *Appl Environ Microbiol* **66**, 5066-+ (2000).
- Porat, I. et al. Characterization of archaeal community in contaminated and uncontaminated surface stream sediments. *Microb Ecol* **60**, 784-795 (2010).
- Francis, C.A., Roberts, K.J., Beman, J.M., Santoro, A.E. & Oakley, B.B. Ubiquity and diversity of ammonia-oxidizing archaea in water columns and sediments of the ocean.

 Proc Natl Acad Sci USA 102, 14683-14688 (2005).
- Peiffer, J.A. et al. Diversity and heritability of the maize rhizosphere microbiome under field conditions. *Proc Natl Acad Sci USA* **110**, 6548-6553 (2013).
- 61. Giardine, B. et al. Galaxy: a platform for interactive large-scale genome analysis. 61. Genome Res 15, 1451-1455 (2005).
- Kong, Y. Btrim: a fast, lightweight adapter and quality trimming program for nextgeneration sequencing technologies. *Genomics* **98**, 152-153 (2011).

- Magoc, T. & Salzberg, S.L. FLASH: fast length adjustment of short reads to improve genome assemblies. *Bioinformatics* **27**, 2957-2963 (2011).
- 829 64. Edgar, R.C. UPARSE: highly accurate OTU sequences from microbial amplicon reads. 830 *Nat Methods* **10**, 996-998 (2013).
- 65. Caporaso, J.G. et al. QIIME allows analysis of high-throughput community sequencing data. *Nat Methods* **7**, 335-336 (2010).
- B33 66. DeSantis, T.Z. et al. Greengenes, a chimera-checked 16S rRNA gene database and workbench compatible with ARB. *Appl Environ Microbiol* **72**, 5069-5072 (2006).
- Wang, Q., Garrity, G.M., Tiedje, J.M. & Cole, J.R. Naive Bayesian classifier for rapid assignment of rRNA sequences into the new bacterial taxonomy. *Appl Environ Microbiol* 73, 5261-5267 (2007).
- 838 68. Edgar, R.C. UNOISE2: improved error-correction for Illumina 16S and ITS amplicon sequencing. *BioRxiv*, 081257 (2016).
- 69. Callahan, B.J. et al. DADA2: High-resolution sample inference from Illumina amplicon data. *Nat Methods* **13**, 581-583 (2016).
- Amir, A. et al. Deblur Rapidly Resolves Single-Nucleotide Community Sequence Patterns. *mSystems* **2** (2017).
- Kembel, S.W. et al. Picante: R tools for integrating phylogenies and ecology. *Bioinformatics* **26**, 1463-1464 (2010).
- Sievers, F. et al. Fast, scalable generation of high-quality protein multiple sequence alignments using Clustal Omega. *Molecular Systems Biology* **7** (2011).
- Price, M.N., Dehal, P.S. & Arkin, A.P. FastTree 2--approximately maximum-likelihood trees for large alignments. *PLoS One* **5**, e9490 (2010).
- Munoz, R. et al. Release LTPs104 of the All-Species Living Tree. *Syst Appl Microbiol* **34**, 169-170 (2011).
- Oksanen, J. et al. Package 'vegan'. *Community ecology package, version* **2.9**, 1-295 (2013).
- Chen, L.X. et al. Comparative metagenomic and metatranscriptomic analyses of microbial communities in acid mine drainage. *ISME J* **9**, 1579-1592 (2015).
- Nakagawa, S. & Schielzeth, H. A general and simple method for obtaining R2 from generalized linear mixed-effects models. *Methods Ecol Evol* **4**, 133-142 (2013).
- Martiny, J.B., Eisen, J.A., Penn, K., Allison, S.D. & Horner-Devine, M.C. Drivers of bacterial beta-diversity depend on spatial scale. *Proc Natl Acad Sci USA* **108**, 7850-7854 (2011).
- Andrews, S. (Babraham Bioinformatics, Babraham Institute, Cambridge, United Kingdom, 2010).
- 863 80. Li, W. & Godzik, A. Cd-hit: a fast program for clustering and comparing large sets of protein or nucleotide sequences. *Bioinformatics* **22**, 1658-1659 (2006).
- Patel, R.K. & Jain, M. NGS QC Toolkit: a toolkit for quality control of next generation sequencing data. *PLoS One* 7, e30619 (2012).
- 867 82. Zhou, J.Z. & Ning, D.L. Stochastic Community Assembly: Does It Matter in Microbial Ecology? *Microbiol Mol Biol R* **81** (2017).
- 869 83. Jaumot, J., Bedia, C. & Tauler, R. Data Analysis for Omic Sciences: Methods and Applications. (Elsevier, 2018).
- 871 84. Thevenot, E.A., Roux, A., Xu, Y., Ezan, E. & Junot, C. Analysis of the Human Adult 872 Urinary Metabolome Variations with Age, Body Mass Index, and Gender by

873	Implementing a Comprehensive Workflow for Univariate and OPLS Statistical Analyses.
874	J Proteome Res 14, 3322-3335 (2015).
875	

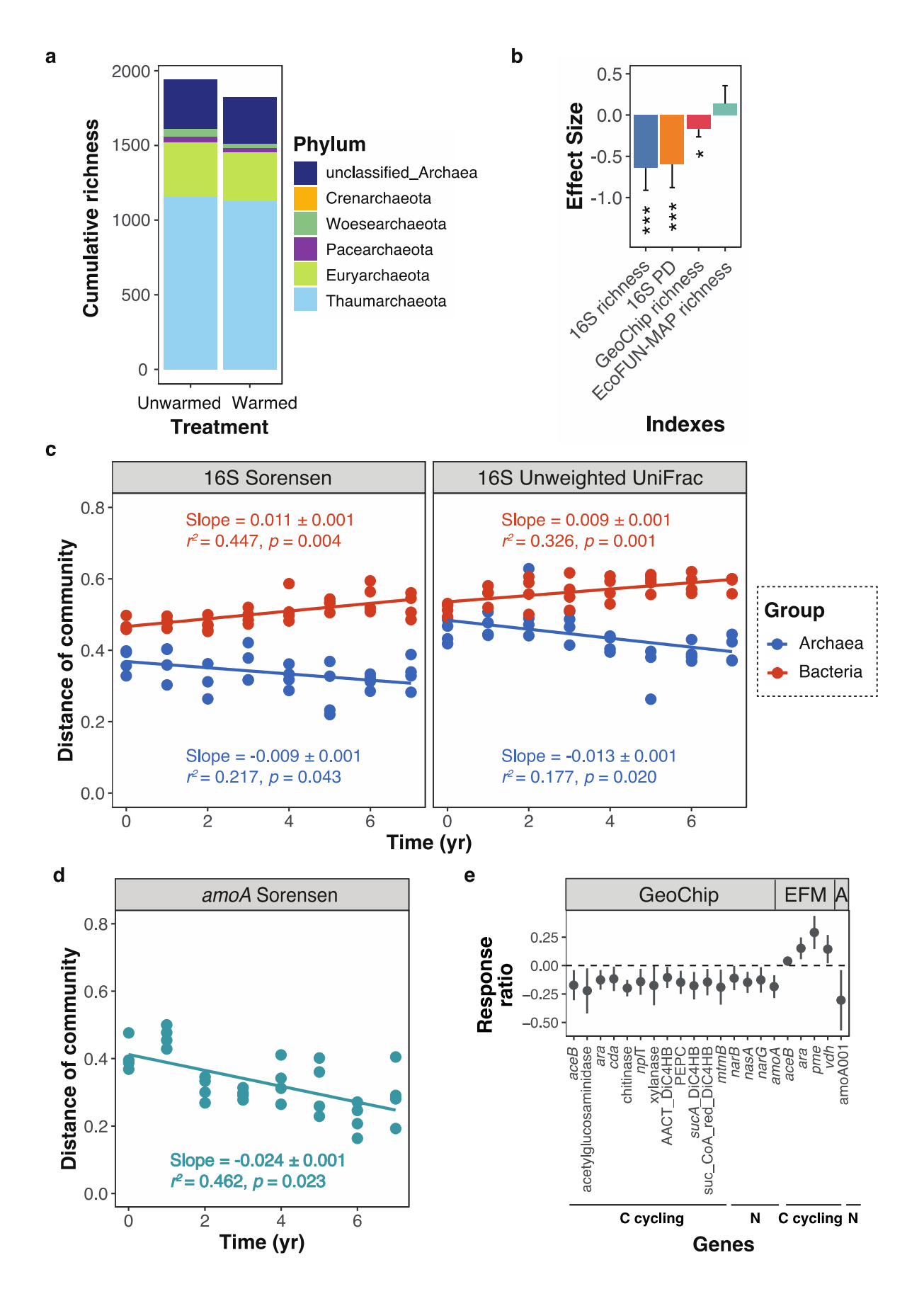


Fig. 1. Effects of experimental warming on the archaeal community diversity and succession across seven years. a, Archaeal community composition under unwarmed and warmed conditions. Cumulative richness is expressed as the number of operational taxonomic units (OTUs). b, The effect sizes of warming on archaeal biodiversity (including taxonomic, phylogenetic, and functional diversity). The estimated effect sizes (β) are regression coefficients based on rescaled response variables (rescaled to one with mean zero and unit standard deviation) in the linear mixed-effects (LMMs) models. Bars represent mean \pm s.e.m. of effect sizes. Statistical significance is based on Wald type II γ^2 tests (n = 64; two-sided; p = 0.008, 0.006, 0.070, 0.533 for 16S richness, 16S PD, GeoChip richness, and EcoFUN-MAP richness, respectively). Significance was expressed as ***p < 0.01; **p < 0.05; *p < 0.10. EcoFUN-MAP is a method designed for annotating metagenomic sequences by comparing them with functional genes used to fabricate GeoChip. c and d, Temporal changes in community differences between warming and control conditions. c, 16S rRNA genes (left: Sorensen dissimilarity metrics; right: unweighted UniFrac dissimilarity metrics); d, amoA genes. The slopes of the archaeal community and the bacterial community are significantly different in c (p = 0.007 and p < 0.0070.001). The first year is 2009 (year 0). Considering the repeated-measures design, the warmingversus-control dissimilarity values at each block were fitted to LMMs with a fixed effect of time and a random intercept and slope effect among different pairs of plots (blocks). The slopes are presented as a coefficient in fixed effect \pm standard error in random effect. The r^2 values are calculated (details in Methods) to reflect the variance explained by the whole LMM model. p values were based on permutation tests (two-sided). The lines showed the fixed effects of the LMM. e. Differences in functional gene abundances between warming and control by response ratios. Bars represent mean \pm 95% confidence interval of response ratios. Only genes showing significant differences between warming and control (p < 0.05, n = 64) are shown. EFM: metagenome EcoFUN-MAP; A: amoA genes (mean relative abundance > 10.0%).

877

878

879

880

881

882

883

884

885

886

887

888

889

890

891

892

893

894

895

896

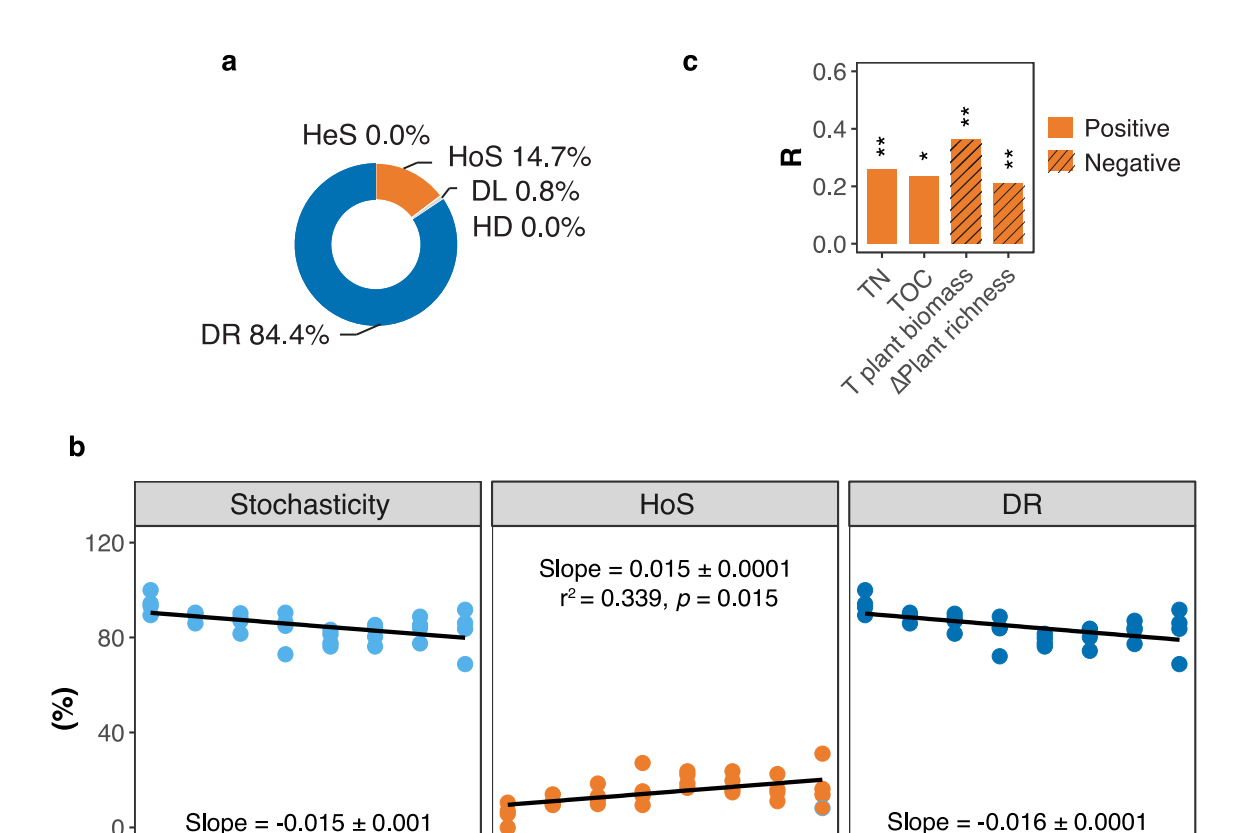
897

898

899

900

901



 $r^2 = 0.327$, p = 0.028

4

6

2

6

ò

0

905 906

907

908

909

910

911

912

913

914

915

916

917

 $r^2 = 0.409$, p = 0.005

2

Fig. 2. Ecological processes and community assembly mechanisms associated with the temporal dynamics in the soil archaeal community. a, Relative importance of deterministic processes (homogeneous selection, HoS; heterogeneous selection, HeS) and stochastic processes (dispersal limitation, DL; homogenizing dispersal, HD; and drift and others, DR) between warming and control treatment. b, Changes in the relative importance of stochastic processes, HoS, and DR (%) between warming and control at each block over the years. Results are based on LMMs (statistical tests and significance are the same as in Fig. 1c-d). c, Effects of environmental factors on deterministic processes defined by the phylogenetic bin-based null model analysis (iCAMP) based on the Mantel test (two-sided). It only shows the factors with significant correlations (p = 0.039, 0.062, 0.049, 0.029 for total N, total organic C, total plant biomass, and the difference of plant richness). See Supplementary Table S7 for other factors. R, coefficient of determination from the Mantel analysis. The correlation was determined based on

Ó

6

2

Time (yr)

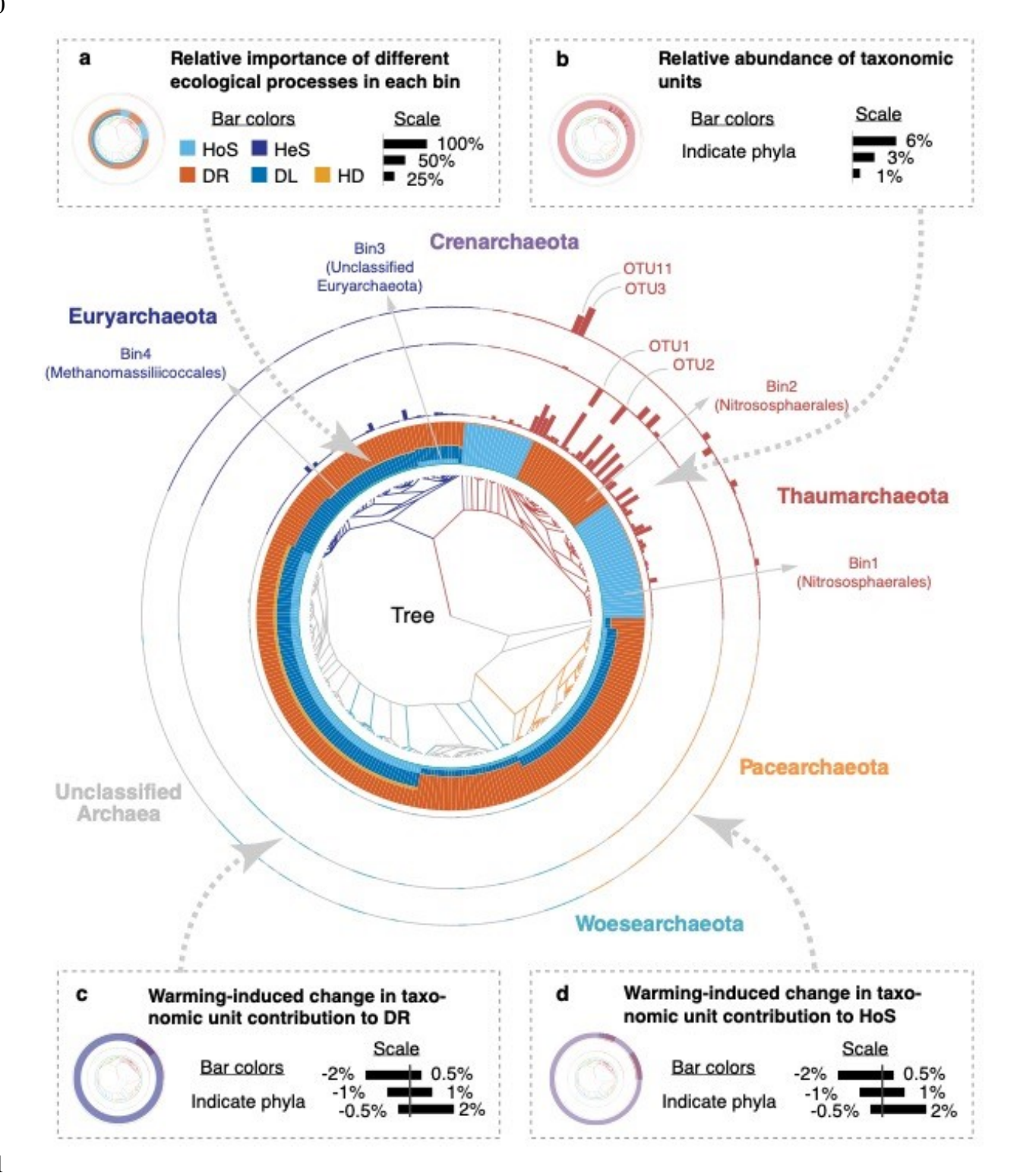
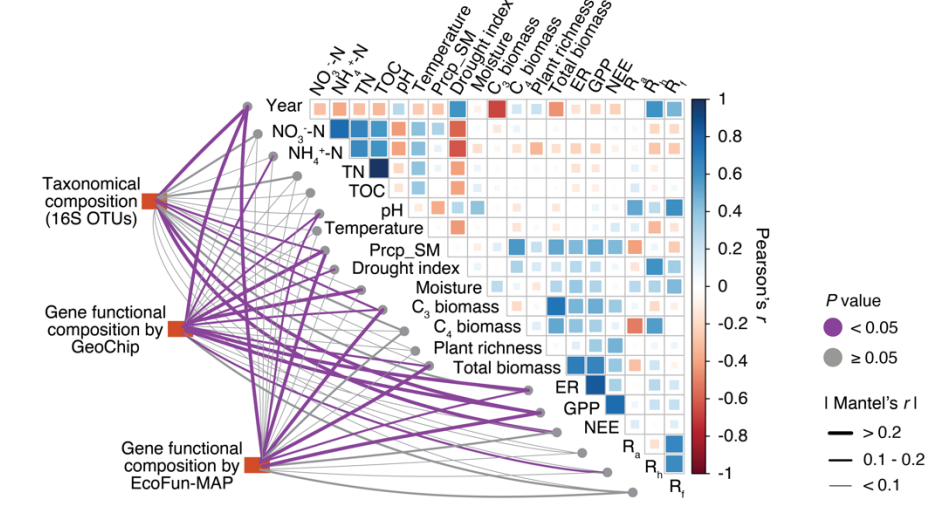


Fig. 3. Variations of ecological processes across different phylogenetic groups. The phylogenetic tree is displayed at the center. **a**, Relative importance of different ecological processes in each bin (stacked bars in the 1st annulus). **b**, Relative abundance of individual taxonomic units (2nd annulus). All 287 taxonomic units are shown. **c**, Warming-induced change in taxonomic unit contribution to drift (3rd annulus), and **d**, homogeneous selection (4th annulus), where positive (outward bar) and negative (inward bar) represented increase and decrease by warming, respectively. The most abundant bins are marked in the figure, including Bin2 (83.5% relative abundance; dominated by Nitrososphaerales), Bin1 (15.1%; Nitrososphaerales), Bin4 (0.9%; Methanomassiliicoccales) and Bin3 (0.2%; unclassified Euryarchaeota).





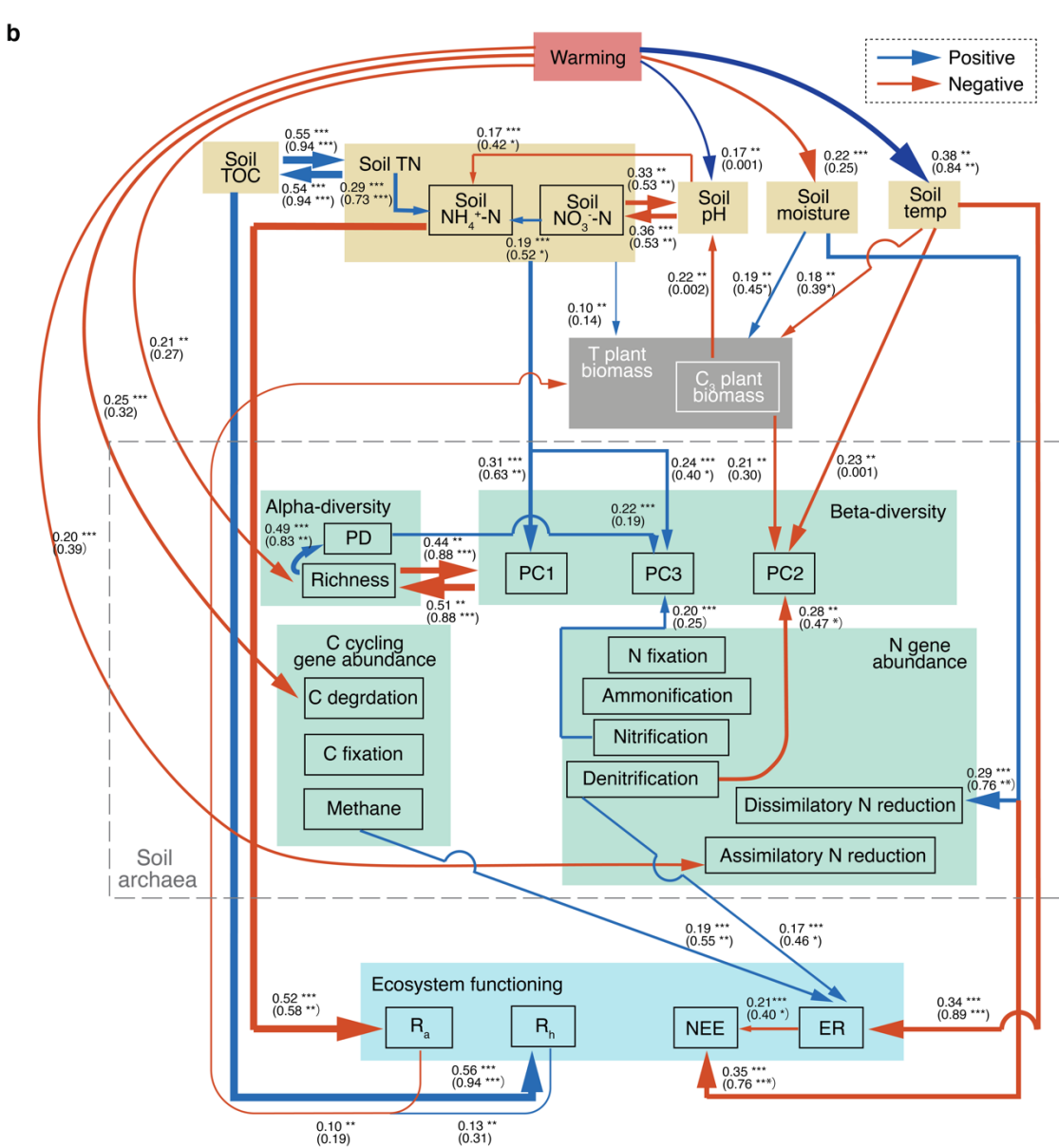


Fig. 4. Environmental drivers of archaeal community structure and functioning. a, Relationships between archaeal community structure and environmental variables and ecosystem processes under warming. See Supplementary Fig. S8 for under control. Archaeal community structures, which include taxonomical composition by 16S rRNA genes and functional gene composition by GeoChip and EcoFUN-MAP, were tested against time, soil and plant variables, and ecosystem C fluxes. The edge width corresponds to Mantel's r value, and the edge color denotes statistical significance (two-sided). Pairwise correlations of these variables are shown with a color gradient denoting Pearson's correlation coefficients. Soil variables include soil nitrate (NO₃-), ammonium (NH₄+), total nitrogen (TN), total organic C (TOC), pH, precipitation of the sampling month (Prep. SM), temperature, moisture, and drought index; plant variables include C₃ and C₄ aboveground biomass, plant richness, and total biomass; ecosystem C fluxes include ecosystem respiration (ER), gross primary productivity (GPP), net ecosystem exchange (NEE), autotrophic respiration (R_a), heterotrophic respiration (R_b), and total soil respiration (R_t). b, Partial least squares (PLS) models on the relationships among treatments (warming), soil properties, plant variables, archaeal community diversity and functional traits, and ecosystem functions. Directions for all arrows are from independent variable(s) to a dependent variable in the forward selected PLS models (p < 0.05 for both R^2_Y and Q^2_Y ; two sided); only the most relevant variables (variable influence on projection > 1) are presented. The numbers near the pathway arrow indicate the proportion of variance explained for every dependent variable, with the top row representing the partial R² index based on PLS (See details in Methods) and the bottom row representing Pearson correlation R². The asterisks denote the significance levels of each optimum PLS model (top row) and Pearson correlation (bottom row). ***p < 0.01, **p < 0.010.05 and *p < 0.10. The widths of pathways are proportional to the partial R² index.

932

933

934

935

936

937

938

939

940

941

942

943

944

945

946

947

948

949

950

951

952

953

954